THE JOURNAL OF PHYSICAL CHEMISTRY B

Article

pubs.acs.org/JPCB

Interaction of L-Phenylalanine with a Phospholipid Monolayer at the Water−Air Interface

Elizabeth C. Griffith,[†] Russell J. Perkins,[†] Dana-Marie Telesford,[‡] Ellen M. Adams,[‡] Lukasz Cwiklik,[§,∥] Heather C. Allen,[‡] Martina Roeselová,*[,∥] and Veronica Vaida*[,†]

[†]Department of Chemistry and Biochemistry and CIRES, University of Colorado at Boulder, UCB 215, Boulder, Colorado 80309, United States

[‡]Department of Chemistry and Biochemistry, The Ohio State University, 100 West 18th Avenue, Columbus, Ohio 43210, United States

[§]J. Heyrovský Institute of Physical Chemistry, Academy of Sciences of the Czech Republic, Dolejškova 3, 18223 Prague 8, Czech Republic

[∥]Institute of Organic Chemistry and Biochemistry, Academy of Sciences of the Czech Republic, Flemingovo nám. 2, 16610 Prague 6, Czech Republic

Supporting Information

ABSTRACT: The interaction of L-phenylalanine with a 1,2-dipalmitoyl-*sn*-glycero-3-phosphocholine (DPPC) monolayer at the air−water interface was explored using a combination of experimental techniques and molecular dynamics (MD) simulations. By means of Langmuir trough methods and Brewster angle microscopy, L-phenylalanine was shown to significantly alter the interfacial tension and the surface domain morphology of the DPPC film. In addition, confocal microscopy was used to explore the aggregation state of L-phenylalanine in the bulk aqueous phase. Finally, MD simulations were performed to gain molecular-level information on the interactions of L-phenylalanine and DPPC at the interface. Taken together, these results show that L-phenylalanine intercalates into a DPPC film at the air−water interface, thereby affecting the surface tension, phase morphology, and ordering of the DPPC film. The results are discussed in the context of biological systems and the mechanism of diseases such as phenylketonuria.

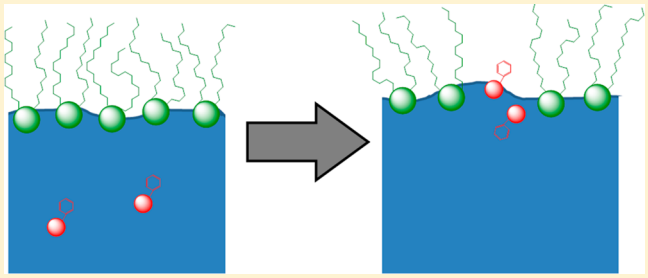

INTRODUCTION

Aromatic residues serve many purposes throughout modern biology[1,2] ranging from playing key roles in membrane channel gating functions[3,4] to the formation of deleterious amyloid structures.[5,6] L-Phenylalanine (Phe) residues in particular have been identified as a key component in the formation of amyloid structures.[7] In general, Phe is a unique molecule in terms of its propensity for self-assembly. Short peptides composed solely of phenylalanine (e.g., Phe-Phe) are known to self-assemble into ordered nanostructures in water.[8] Furthermore, the monomer amino acid has recently been suggested to self-assemble into amyloid-like fibrils that are proposed to play a role in cytotoxicity relevant to the disease phenylketonuria (PKU).[9,10] On the other hand, the process of polypeptide fibrillization was shown to be modulated by lipid−peptide interactions and to be able to disturb membrane function.[11,12]

Despite the vast knowledge currently being amassed on the many functions of aromatic residues and even single aromatic amino acids, it is still quite difficult to obtain molecular-level information on the causes and mechanisms of these functions. To aid in the molecular-level description of interactions involving biological lipid membranes, the simplified model system of a monolayer at the air−water interface is often used rather than the bilayer structure found in natural biological systems.[13−19] Despite being a model system (neglecting, for instance, the presence of proteins, membrane asymmetry, and curvature effects), monolayers have the same lipid−water interface present in bilayer systems and thus allow the exploration of perturbations to the membrane caused by changes in the composition of the aqueous phase or penetration of various compounds into the lipid phase. In addition, using a monolayer rather than a bilayer has many advantages, allowing for greater ease in control of both experimental and simulation conditions.[20,21] Here a 1,2-dipalmitoyl-*sn*-glycero-3-phosphocholine (DPPC) monolayer is used as a model system to explore the interactions of Phe with a phospholipid membrane in order to gain molecular-level information not traditionally available to more phenomenological molecular biology studies. DPPC was chosen because it

Special Issue: Branka M. Ladanyi Festschrift

Received: August 21, 2014
Revised: December 8, 2014
Published: December 9, 2014

DOI: 10.1021/jp508473w
J. Phys. Chem. B 2015, 119, 9038−9048

is one of the best experimentally and computationally characterized lipids that is also biologically relevant (phosphatidylcholines are the major class of lipids found in mammalian cell membranes, and DPPC itself is the main lipid component of lung surfactants).[21−26]

The interactions between interfacial molecules with varying hydrophobic structure are important in many fields ranging from atmospheric chemistry to biological and medicinal chemistry.[14−17,19,27−32] In previous work, aromatic soluble surfactants (Phe, benzoic acid, and benzaldehyde) have been shown to affect surface morphology and even to disrupt the stability of a monolayer of insoluble fatty acid surfactant (stearic acid) at the water−air interface depending on the headgroup structure of the aromatic species.[28,29] Among the aromatic species explored, Phe caused complete destabilization of the fatty acid film,[28] whereas benzoic acid and benzaldehyde[29] exhibited only evidence of interaction and small modification of the fatty acid monolayer at the water surface. In this work, the interaction of Phe with a phospholipid (DPPC) monolayer at the air−water interface is explored with complementary information obtained through experiment (using Langmuir trough methods and Brewster angle microscopy (BAM)) and molecular dynamics (MD) simulations. In addition, the aggregation of L-phenylalanine in the bulk aqueous phase is studied using confocal microscopy.

The recent work by Adler-Abramovich et al.[9] is intriguing in this context. They reported the self-assembly of Phe monomers into long fibrils that were subsequently observed to be cytotoxic, even resulting in misshapen cells for the remaining viable cells. This effect is very important in understanding the cause of PKU, which is characterized by an inability to process ingested phenylalanine. However, no mechanistic insight into this cytotoxicity has been obtained to date beyond the assertion of the apparent similarity to amyloid structures. Thus, the aim of this work is to gain insight into the molecular-level interactions of Phe with a model phospholipid−water interface characteristic of cell membranes. This will aid in understanding not only the mechanism of the cytotoxicity of Phe in PKU but also the interactions of other Phe-rich aggregates found in biology with cell membranes.

MATERIALS AND METHODS

All materials were purchased and used without further purification. Phe was purchased from Alfa Aesar (99%) and was dissolved in deionized (DI) water to a final concentration of 2.5 mM for the pre-equilibrated subphase experiments and 115 mM for the injection experiments (pre-equilibrated DPPC monolayer experiments; see below). The pH of DI water was measured at 5.5, indicating that the zwitterionic state of Phe would dominate in bulk solution as well as near the air−water interface in the absence of DPPC.[33] The solution was prepared fresh for each experiment. It is important to note that there was a difference found in the purity of commercial Phe that affected the rate of adsorption to the surface. However, the overall effects observed remained consistent. DPPC (>99%, purchased from Sigma-Aldrich for Langmuir trough experiments and from Avanti, lot no. 223938, for BAM experiments) was dissolved in chloroform (ACS grade, Mallinckrodt Baker) to a final concentration of 1.6 mg/mL to be deposited dropwise onto the aqueous subphase in the Langmuir trough in the subsequent experiments.

Two different experiments were performed using the Langmuir trough and BAM: one with a pre-equilibrated subphase containing Phe and one with a pre-equilibrated DPPC monolayer. In the pre-equilibrated subphase experiment, a 2.5 mM solution of Phe was prepared and spread on the Langmuir trough. Then DPPC was deposited on the equilibrated subphase at a molecular area of 70 Å^2/molecule. In the pre-equilibrated DPPC monolayer experiments, DPPC was deposited dropwise on a neat water surface to a molecular area of 70 Å^2/molecule, allowing DPPC to form a stable monolayer. Then 2 mL of the 115 mM solution of Phe (in the small Langmuir trough described in the BAM experiments) was slowly injected beneath the DPPC-covered water surface.

Langmuir Trough. Langmuir trough methods were used to monitor and characterize the phase behavior of the mixed film system. The Langmuir trough used was custom-built (52 cm × 7 cm × 0.5 cm) and consisted of a PTFE trough as well as two PTFE barriers controlled by software purchased from NIMA (KSV-NIMA, Finland). This trough was coupled to a Wilhelmy balance used to measure the surface pressure (π), i.e., the decrease in surface tension. When the PTFE barriers are moved, surface pressure−area (π−A) isotherms can be produced, or the barriers can be held stationary to record surface pressure−time (π−t) adsorption isotherms. These isotherms yield surface thermodynamic information that allows monitoring of changes in the phase behavior of the surfactant of interest (DPPC) in the presence of the perturbant (Phe).

Brewster Angle Microscopy. BAM is a useful tool to visualize morphological changes on a microscopic scale (approximately 500 μm × 500 μm image size) at the water surface.[34,35] BAM images were collected by illuminating the water surface in the Langmuir trough (8.34 cm × 16.90 cm) at the Brewster angle of water (53°) and magnifying the reflected image before collection with a camera. The illumination source was a 5 mW polarized 543 nm laser (Research Electro-Optics) that was passed through a half-wave plate and a Glan−Thompson polarizer for attenuation and p polarization relative to the water surface. The reflection was magnified using a Nikon 10× infinity-corrected superlong working distance objective and corresponding tube lens. The camera was a back-illuminated electron-multiplying charge-coupled device (CCD) (Andor iXon model DV887-BV, 512 × 512 pixels). BAM images were obtained every 5 min.

Microscopy. Confocal microscopy images of 120 mM Phe dyed with 0.2 mM thioflavin T (ThT) were taken using a Nikon A1R confocal microscope with a 100× (NA 1.45) Plan Apochromatic objective. The sample was prepared by adding 100 μL of 40 mM ThT dye to a 20 mL volume of Phe and then depositing a 10−20 μL drop on a precleaned glass coverslip prior to illumination with a 457.9 nm laser. Emission from the sample was filtered with a 482/35 nm bandpass filter prior to collection with an iXon X3 EMCCD camera.

Molecular Dynamics Simulations. Classical MD simulations were performed for three different systems, each composed of two monolayers of DPPC (64 molecules each), one on either side of an aqueous slab, placed in the middle of a 6.69 nm × 6.69 nm × 28 nm simulation box. Periodic boundary conditions were used in all directions. The thickness of the entire slab system (including the two DPPC monolayers) was approximately 7 nm, leaving about 21 nm of vacuum between the periodic images in the z direction normal to the aqueous slab−DPPC interface. In the three systems simulated, the aqueous slab was composed of water, water containing zwitterionic Phe molecules, and water containing neutral Phe molecules. Although Phe does exist in its zwitterionic form in

DOI: 10.1021/jp508473w
J. Phys. Chem. B 2015, 119, 9038−9048

aqueous solution at physiologically relevant pH, it could transition to its neutral form in the relatively nonpolar core of the phospholipid bilayer, as has been seen with other membrane-perturbing molecules.[36,37] Phe itself has been seen to alter its ionization state at the air−water interface,[33] allowing for the possibility of its alteration at the membrane interface. Thus, both situations (i.e., zwitterionic as well as neutral Phe) were simulated and subsequently analyzed. Each system is described in more detail below.

(a). DPPC Monolayer on Water. The system consisted of two monolayers of DPPC (64 molecules each) solvated with a slab containing 6876 water molecules. The system was created from a previously equilibrated (50 ns, *NPT* ensemble, P = 1 bar, T = 310 K) lipid bilayer of 128 DPPC molecules (64 in each leaflet) by applying the following procedure. The size of the periodic box used in the bilayer−water simulation was increased 3-fold in the direction of the bilayer normal. Then the two lipid leaflets with their hydrating water layers were rearranged by translating them along the bilayer normal to create two monolayers, one at each surface of a water slab. The resulting system was equilibrated for 10 ns in the *NVT* ensemble at T = 310 K. Then a negative lateral pressure (−25 bar) was employed in the *NPT* ensemble in a short (<1 ns) simulation in order to laterally decompress the system and hence to obtain the desired area per lipid of 70 Å^2/molecule. The resulting simulation box had the dimensions of 6.69 nm × 6.69 nm × 28.0 nm. The system was further equilibrated in the *NVT* ensemble for 50 ns at T = 310 K. This was followed by a 50 ns trajectory that was used for analysis.

(b). Zwitterionic Phe/DPPC System. The initial DPPC monolayer configuration was taken from the equilibrated configuration described in the previous section. The aqueous slab containing 20 zwitterionic Phe molecules distributed randomly and solvated with water molecules was then inserted between the two hydrated DPPC monolayers (the insertion procedure is described in more detail in the Supporting Information), resulting in a total of 5531 water molecules in the system. This corresponds to an initial Phe concentration of 200 mM in the aqueous solution slab separating the two DPPC monolayers. A short energy minimization was first run, after which the newly created system was equilibrated for 10 ns in the *NVT* ensemble at T = 310 K and then propagated for 100 ns (see below). After completion of the 100 ns production run, most of the Phe molecules had partitioned into the interfacial regions, leaving only 5−10% of the initial Phe molecules in the bulk aqueous phase. Thus, a second simulation (100 ns) was performed with 15 additional molecules of zwitterionic Phe added to the interior of the aqueous slab (following the same insertion procedure described for the initial insertion of Phe) to more closely mimic the experimental conditions, in which a nearly continuous supply of monomers is provided to the interfacial region from the macroscopic bulk phase. The last 50 ns of each of the two simulations (with 20 and 35 Phe molecules) was used for analysis.

(c). Neutral Phe/DPPC System. The system was prepared following the same procedure as for the zwitterionic Phe/DPPC system, with the initial DPPC monolayer configuration again taken from the equilibrated configuration described above. The final composition of the aqueous portion of the system was 20 neutral Phe molecules distributed randomly and solvated with 5613 water molecules between the DPPC monolayers. This corresponds to an initial concentration of 198 mM Phe in the aqueous phase of the system. As in the previous case, a short energy minimization was first run, followed by a 10 ns equilibration period. Then a 100 ns production run was completed, of which the last 50 ns was used for analysis.

All of the simulations were performed in the isochoric−isothermal (*NVT*) ensemble at a temperature of 310 K. The Nosé−Hoover thermostat[38,39] with a time constant of 0.5 ps was used for temperature control. The equations of motion were integrated utilizing the leapfrog algorithm[40] with a time step of 2 fs, and snapshots were saved every 10 ps. A cutoff distance of 1 nm was used for the Lennard-Jones potential and the short-range part of the electrostatic interactions, and the long-range part of the electrostatic interactions was treated using the particle-mesh Ewald scheme.[41] All of the bond lengths were constrained using the LINCS algorithm.[42] Simulations were run and analyzed using GROMACS version 4.6.3[43] and visualized using VMD.[44]

The SLipids force field[45,46] was used for the DPPC molecules, while the TIP3P model (the default water model for SLipids) was employed for water molecules. Standard DPPC force field parameters were obtained from http://people.su.se/~jjm/Stockholm_Lipids/Downloads_files/DPPC.itp, with many parameters coming from CHARMM36.[47] Phe molecules were modeled using the Amber ff03[48,49] force field. The atomic partial charges of both the zwitterionic and neutral forms of Phe were calculated by geometry optimization at the B3LYP/cc-pVTZ level of theory followed by restrained electrostatic potential (RESP) fitting.[50] For zwitterionic Phe, the geometry optimization was carried out including implicit solvation using the polarizable continuum model (PCM).[51] All of the ab initio calculations were conducted using the Gaussian 09 package,[52] and the RESP calculations were performed using Antechamber.[53] The atomic types and charges of both zwitterionic and neutral Phe are given in Tables S1 and S2 in the Supporting Information. The molecular structures of Phe and DPPC with numbering of atoms are shown in Figure 1. The topology files containing all of the force field parameters used in this work are also available in the Supporting Information.

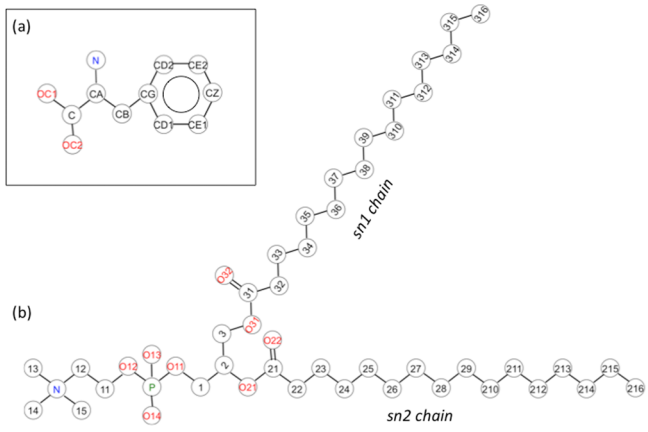

Figure 1. Molecular structures and numbering of atoms for (a) Phe and (b) DPPC used in the MD simulations and analysis. The carbon atoms in the DPPC molecule are shown with numbers only, and all of the hydrogen atoms have been removed for clarity.

DOI: 10.1021/jp508473w
J. Phys. Chem. B 2015, 119, 9038−9048

RESULTS AND DISCUSSION

In the following, both experimental and MD simulation results are presented for the system composed of L-phenylalanine (Phe) dissolved in water in the presence of a DPPC monomolecular surface film. In classical PKU, blood Phe concentrations exceed 1.2 mM, and prolonged exposure is associated with growth defects, seizures, and intellectual impairment.[54] The concentration of Phe used in the following experiments was 2.5 mM in order to mimic the damaging disease state, or higher when no effect was observed at low concentration. Langmuir trough methods and Brewster angle microscopy (BAM) were used to explore the effect of Phe on the phase behavior of DPPC at a molecular area representative of cell membranes (70 Å^2/molecule).[55] Confocal microscopy was then used to explore the aggregation state of Phe in solution. In addition, MD simulations were used to gain insight into the interactions between the Phe molecules and the DPPC film as well as the effect of the intercalation of Phe on the DPPC film itself.

(i). Influence of L-Phenylalanine on Surface Tension. The red curve in the inset of Figure 2 shows the adsorption of Phe to a bare water−air interface, manifested as a mild increase in surface pressure over time measured for 2.5 mM Phe solution. In contrast, when DPPC was deposited on a subphase of aqueous Phe (2.5 mM) at a molecular area of 70 Å^2/molecule, there was a significant rise in surface pressure over time (black curve, Figure 2inset), indicative of much stronger adsorption of Phe to the DPPC-covered interfacial region.[28] Of some interest is the long time scale observed for the saturation of the interface, suggesting that a process other than simple diffusive equilibration is important. Once saturation of the interfacial region was reached for the DPPC-coated interface (indicated by a constant surface pressure), a surface pressure−area (π−A) compression isotherm was obtained (black curve, Figure 2). From a comparison with a π−A isotherm of DPPC deposited on a neat water subphase (blue curve, Figure 2), which exhibits the well-known phase changes of DPPC monolayers at the water surface,[26] it is apparent that there is a change in the phase behavior of DPPC due to the presence of Phe. In the case of the DPPC film on pure water, the π−A isotherm was measured starting from a large molecular area corresponding to the liquid expanded−gas coexistence region of the DPPC monolayer. Upon compression, the film transitions to a liquid expanded (LE) phase around 100 Å^2/molecule. Then the plateau between 80 and 60 Å^2/molecule indicates the liquid expanded−liquid condensed (LE−LC) coexistence region, the region representative of the phase experienced by phospholipids in cell membranes.[55] Finally, the film transitions to a pure LC phase around 55 Å^2/molecule. For the DPPC film on the Phe solution subphase, however, an increased equilibrium surface pressure is measured (~25 mN/m after Phe adsorption compared with ~6 mN/m for DPPC on the water subphase), indicating perturbation of the LE−LC coexistence region of the DPPC film. This is followed by a transition to the LC phase at ~48 Å^2/molecule. The increase in surface pressure of the DPPC film on the Phe solution subphase with respect to the water subphase in the region between 70 and 48 Å^2/molecule is attributed to the presence of Phe in the interfacial region.

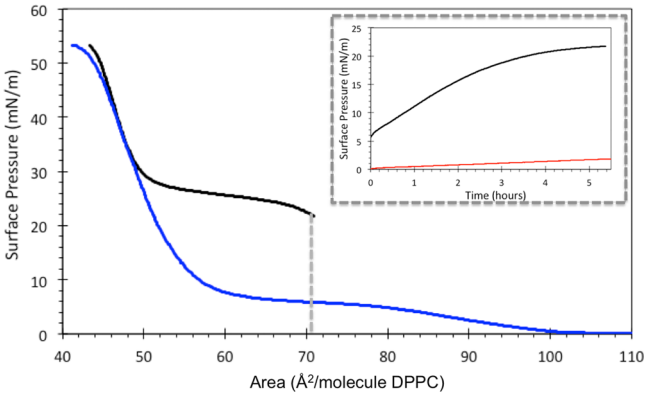

Figure 2. π−A isotherms of DPPC deposited on a neat water surface (blue) and DPPC deposited on a 2.5 mM aqueous solution of Phe (black). The inset shows the adsorption of Phe to the DPPC-covered interface over time at mean molecular area of 70 Å^2/molecule (in the region indicated by the gray dotted line in the π−A isotherms) prior to surface compression (black) as well as adsorption of Phe to a bare aqueous interface over time at the same concentration (2.5 mM) for comparison (red).

The change in surface tension due to the presence of Phe as illustrated in Figure 2 can have significant consequences for the stability and morphology of a cell membrane. For example, regions of differing surface tension on the cell-membrane surface can induce changes in the cell shape and can even cause the membrane to rupture.[56,57] The results presented here in conjunction with those of Adler-Abramovich et al.[9] suggest that this decrease in surface tension induced by the presence of Phe in the interfacial region contributes to the cytotoxicity as well as the change in cell morphology observed.

(ii). Partitioning of L-Phenylalanine at the Aqueous−DPPC Interface. The isotherms shown above (Figure 2) indicate the presence of Phe in the DPPC-covered interfacial region. However, no information can be gained from the isotherms as to whether the Phe molecules are strictly partitioned to the lipid−water interface under the lipid film or intercalated into the lipid film. To gain further insight into the details of Phe interactions with the DPPC film, MD simulations of the mixed film system were used, beginning with Phe molecules solvated in the bulk aqueous phase in the presence of an interface coated with DPPC molecules at a mean molecular area of 70 Å^2/molecule (LE−LC coexistence region, representative of cell membranes[55]). Both zwitterionic and neutral Phe were simulated. Although Phe would exist in a zwitterionic state in pure water, the transition to a neutral state would be possible within the phospholipid membrane. Both systems were examined in order to determine what changes would be expected if this transition were to occur.

Visual inspection of the trajectories reveals that both neutral and zwitterionic Phe diffuse within the aqueous phase at the start of the simulation, forming short-lived small clusters in the aqueous phase ranging from approximately two to five monomers in size (see Figure S2 in the Supporting Information for characteristic snapshots of both simulations during adsorption). As the trajectories progress, molecules of both ionization states interact with the DPPC monolayers. The neutral Phe molecules quickly intercalate into the film and remain inside the film for the rest of the simulation, never returning to the aqueous phase, thus depleting the aqueous phase of all Phe molecules. The zwitterionic Phe molecules are much more dynamic, however, interacting with and even intercalating into the DPPC film but subsequently returning back into the bulk aqueous phase. However, even in the case of

DOI: 10.1021/jp508473w
J. Phys. Chem. B 2015, 119, 9038−9048

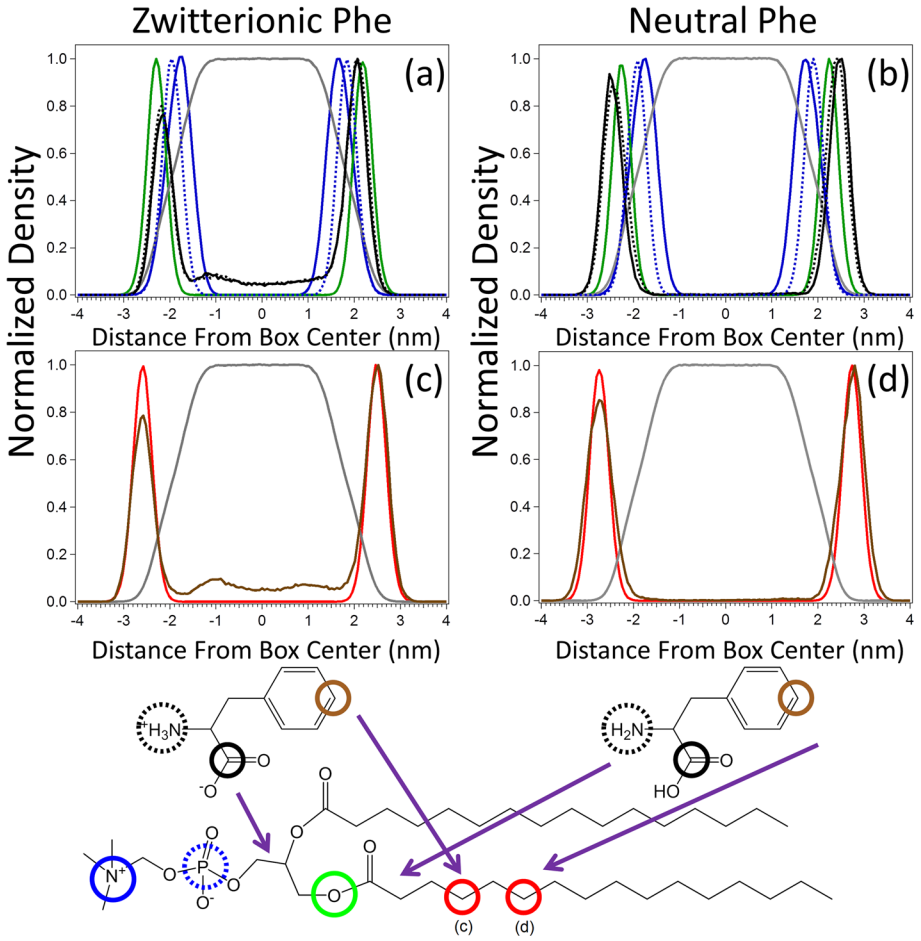

Figure 3. Density profiles illustrating average positioning of Phe (20 molecules) during the last 50 ns of simulation time (100 ns total) in comparison with DPPC density profiles. (a) and (c) are from the simulations with zwitterionic Phe, and (b) and (d) are from the neutral Phe simulations (the corresponding structures are shown at the bottom). The gray curve in each panel corresponds to the density profile of water. The cartoon at the bottom highlights atoms graphed above in matching colors. Purple arrows indicate rough positions of the labeled atoms based on the density profiles. Color coding for Phe: black solid lines, C (carboxyl group); black dotted lines, N (amine group); brown lines, CZ (aromatic ring). For DPPC: blue solid lines, N (choline group); blue dotted lines, P (phosphate group); green lines, O21 (carbonyl groups); red lines, C24 in (c) and C26 in (d).

the zwitterionic Phe molecules, as the trajectory progresses a majority of Phe molecules remain embedded within the DPPC monolayers. Molecules of both ionization states primarily intercalate as monomers, but dimer clusters were also observed within the film. With the addition of 15 zwitterionic Phe molecules to the original 20 Phe zwitterions after the initial 100 ns simulation, the same behavior was observed in the following 100 ns run as described above, with the exception that larger clusters (reaching three and four monomers in size) were observed within the film toward the end of the trajectory.

To ascertain the average positioning of the Phe molecules in the interfacial region, density profiles along the direction normal to the DPPC interface were calculated, and the results are shown in Figure 3a,c for the zwitterionic Phe/DPPC system and Figure 3b,d for the neutral Phe/DPPC system. Both sets of density profiles were computed from the simulations with 20 Phe molecules; density profiles for zwitterionic Phe evaluated from the additional simulation with 35 Phe molecules yielded the same results and are therefore not shown here. In the top panels (Figure 3a,b), the density profiles of the polar head groups are compared. In the bottom panels (Figure 3c,d), the density profiles of the terminal ring carbon of Phe (CZ in the molecular scheme shown in Figure 1a) are matched with the closest density profiles of carbon atoms in the hydrocarbon tails of DPPC (shown in red).

From the density profiles it can be concluded that zwitterionic Phe is positioned, on average, with its headgroup between the phosphate group of DPPC (P) and O21/O31 on the sn2/sn1 chains. The density profiles for the corresponding atoms on the two chains are nearly identical, and thus, only the atoms from the sn2 chain are shown here. The aromatic group of zwitterionic Phe does penetrate between the hydrocarbon tails of DPPC, with the density profile of CZ of Phe overlapping most closely with the density profile of C24 in DPPC. Neutral Phe penetrates deeper into the DPPC film compared to the zwitterion, with the neutral headgroup positioned on average beyond the O21/O31 region of DPPC and CZ as deep as C26 in the DPPC hydrocarbon tail.

The above findings inferred from the density profiles were further corroborated by visual inspection of the trajectories, which revealed that neutral Phe molecules can change their orientation within the film, dehydrating their polar groups and embedding deeper into the nonpolar phase (see Figure S3 in the Supporting Information). Zwitterionic Phe, however, remains with its polar groups hydrated and anchored in the aqueous region of the interface. This suggests that if Phe does transition to its neutral state upon entering the phospholipid

DOI: 10.1021/jp508473w
J. Phys. Chem. B 2015, 119, 9038−9048

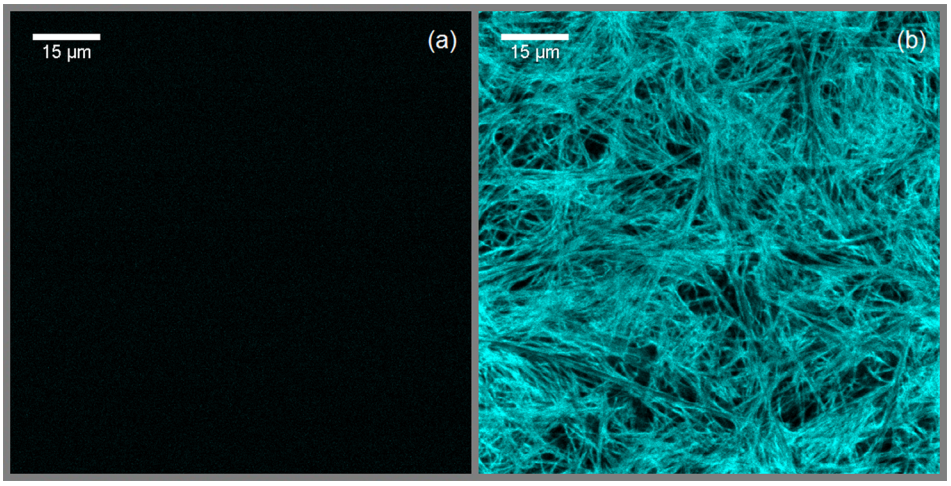

Figure 4. Confocal microscopy images of 120 mM Phe stained with ThT. (a) Image of Phe in aqueous solution (this panel is mostly black, with small dots corresponding to free dye but no structures). (b) Refocused image of the same spot as in (a) after drying, with the same imaging contrast. Scale bars represent 15 μm.

film, it can penetrate rather deeply between the DPPC molecules, well into the hydrophobic region of the monolayer. Although this is a monolayer study and membrane crossing events are impossible here, the dehydration and deeper penetration of neutral Phe into the nonpolar region of the phospholipid monolayer opens the possibility for such crossing events in a bilayer system.

(iii). Aggregation State of Phe in Solution. It has been suggested in the literature that Phe forms large amyloid-like fibrils in solution, which are proposed to be responsible for the cytotoxicity observed in PKU.[9,10] Throughout the simulations performed in this work, small clusters of Phe molecules (in both the neutral and zwitterionic simulations) were observed in the bulk and interfacial regions in the presence of DPPC, but they were rather short-lived, and no long fibril-like structures were observed. The extent of aggregation of amino acids can be dependent upon the force field chosen for the simulations,[58] and thus, the formation of fibrils was also explored experimentally here using confocal microscopy and staining with thioflavin T (ThT). As shown below in Figure 4a, no fibrils were observed in solution, even at the high concentration of 120 mM. However, upon drying of the solution (presumably yielding a supersaturated solution with a concentration of >153 mM[59]), crystallization occurred in the same viewpoint (Figure 4b; see Figure S4 in the Supporting Information for the time evolution of crystallization with drying), yielding structures comparable to those in samples prepared under similar conditions and reported in the literature as amyloid-like fibrils.[9,10]

Furthermore, at lower concentrations (2.5 mM Phe; Figure S5 in the Supporting Information) similar crystal formation occurs and appears to begin at the periphery of the drop as it dries. In contrast to the bulk solution images, some aggregates were also observed in BAM images of 2.5−20 mM Phe on a bare water surface (Figure S6 in the Supporting Information). The experimental findings presented indicate that most of the Phe in pure bulk solution, even at the relatively high physiological concentrations present in a diseased state, does not exist as long fibril-like aggregates; instead, fibril formation occurs upon a significant increase in concentration or interactions with the interface. The special environment provided by an interface has been previously suggested to be important in many different contexts, ranging from influencing the ionization state of molecules to promoting chemistry not available in the bulk aqueous environment.[13,33,60−62] Here the surface is implicated in promoting aggregation through increased local concentrations and interactions of Phe with the interface. It is important to note that in these studies no ions were present in solution as is the case in biological systems and as have been used in previous studies.[9] The addition of salt to the system could also influence the aggregation and interactions of Phe.

The absence of Phe aggregate formation in the bulk solution is important in terms of the interaction of Phe with a biological membrane. Despite the fact that Phe is dilute in the bulk aqueous environment at biologically relevant concentrations, it does accumulate in the interfacial region, as evidenced here by the surface tension data as well as the MD simulations. Thus, in the interfacial region, much higher concentrations of Phe may be reached, increasing the likelihood of more extended aggregation in the specific, special environment provided by the phospholipid interface. Additionally, an interfacial aggregation phenomenon would be consistent with the long-time-scale saturation effects observed in Phe surface adsorption experiments (i.e., the nondiffusive process mentioned earlier), although it is possible that this long-time-scale saturation is due to another slow process, such as intercalation into the membrane or a change in ionization state. Interestingly, phospholipid−water interfaces have been shown to promote aggregation of a variety of peptide sequences[11,12,63−65] through increased local concentration and two-dimensional diffusion when the peptides are bound to phospholipid membranes.[66] One specific example is the toxic misfolding of human islet amyloid polypeptide (hIAPP).[67] hIAPP is a naturally disordered protein that forms ordered structures through interaction with a membrane; in general, the misfolding of naturally disordered proteins is thought to be a contributing factor in diseases such as Alzheimer's, Parkinson's and type-II diabetes.[68−70] It is possible that the membrane plays a similar role here, indeed enhancing the aggregation of Phe and contributing to the cytotoxicity associated with PKU and observed in other studies.[9]

(iv). Morphological and Ordering Effect of Phe on the DPPC Film. Beyond understanding the intercalation of Phe

DOI: 10.1021/jp508473w
J. Phys. Chem. B 2015, 119, 9038−9048

into the DPPC monolayer, it is important in a biological context to understand the effect this intercalation has on the DPPC film itself. The domain morphology of a DPPC film is one good way to experimentally gain insight into the effect of additives such as Phe on a phospholipid membrane.[24] BAM images of DPPC deposited on water, on an aqueous subphase of 2.5 mM Phe, and on water followed by injection of Phe beneath the surface layer are shown in Figure 5a−c, respectively.

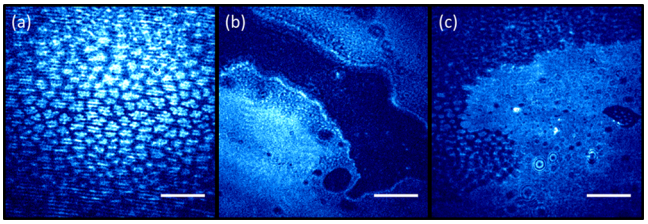

Figure 5. BAM images of DPPC deposited at 70 Å^2/molecule (a) on a neat water surface, (b) on an aqueous subphase composed of 2.5 mM Phe, and (c) on a neat water subphase followed by injection of Phe beneath the water surface. Scale bars represent 100 μm. The image in (b) was collected approximately 5 min after deposition, and the image in (c) was collected approximately 2 h 51 min after injection.

On a bare water subphase (Figure 5a), DPPC exhibits the characteristic island structure formed in the LE−LC coexistence region of its π−A isotherm (BAM images of DPPC in various phases throughout its π−A isotherm are shown in Figure S7 in the Supporting Information).[24] However, when deposited on a subphase containing Phe (Figure 5b), DPPC exhibits extended condensed domains along with ribbons and circular domains of lesser DPPC coverage. Deposition on a subphase containing Phe molecules resulted in immediate domain morphology changes that were stable over time. Despite this immediate perturbation, the initial surface tension recorded upon spreading of DPPC at the surface was identical in the presence and absence of Phe in the subphase (the initial surface pressure upon spreading at 70 Å^2/molecule both on a bare water surface and on an aqueous Phe solution was consistent at ∼6 mN/m), indicating that although the film was perturbed, it was still able to attain a similar surface pressure. However, to confirm that the pre-existence of Phe in the subphase did not cause an artificial change in domain morphology due to different spreading behavior, an injection experiment was also performed. In this experiment, DPPC was deposited on a water surface, forming its characteristic domain structure as shown in Figure 5a. Then Phe was injected beneath the surface layer, and the resulting BAM image is shown in Figure 5c. As in Figure 5b, large condensed domains were also observed in the injection experiment as well as domains of lesser surfactant coverage. However, in both cases (Figure 5b,c) there were also still some domains observed with the characteristic island structure of DPPC in the LE−LC phase region. Thus, regardless of whether the DPPC or Phe solution is initially equilibrated, similar perturbations due to Phe yielding a change in the DPPC film morphology are observed. Because of the heterogeneity of the mixed films in regions larger than the images (approximately 500 μm × 500 μm) and morphological changes observed within minutes of Phe exposure, no useful information could be gathered about morphological changes over time. Because of this, images were chosen to be representative of the observed morphologies rather than for temporal significance.

This experimental effect was supported by the simulation results, in which small voids were periodically formed in the DPPC film in the presence of zwitterionic Phe. One snapshot showing this effect is presented in Figure 6, with the void in the

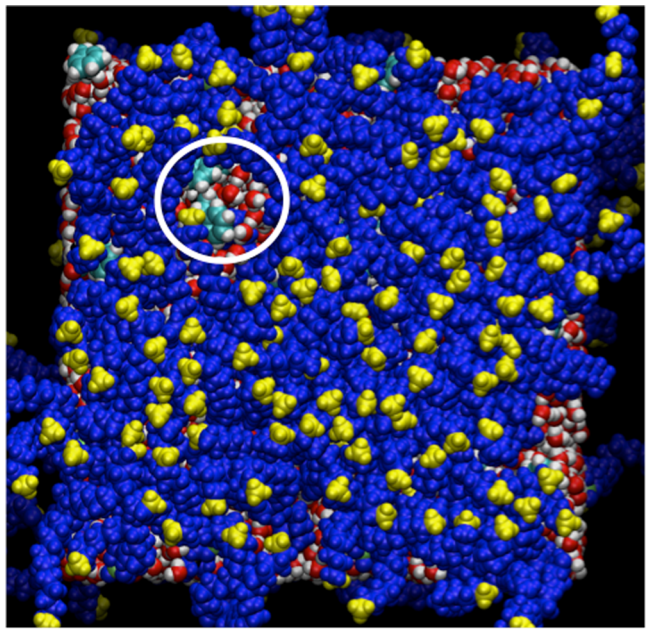

Figure 6. Top-view snapshot of a small-scale defect in the DPPC film from an MD simulation (defect circled in white). DPPC molecules are colored blue with terminal methyl groups colored yellow. Water molecules are red and white, and Phe molecules can be seen by their green aromatic rings.

film circled in white. The proximity and ordering of the terminal methyl groups of DPPC (colored in yellow in Figure 6) can be used as an indicator of condensed domains in the film.[71] In conjunction with periodic voids formed in the monolayer like the one shown in Figure 6, regions of condensed film (seen as clusters of yellow terminal methyl groups) were also visually observed throughout the simulation.

To quantify the visual condensing effect of Phe on the DPPC monolayer observed in the MD simulations, deuterium order parameters were calculated,[72] and the results are presented in Figure 7. The deuterium order parameter is typically used to characterize the order in acyl chains and can be also obtained experimentally from deuterium NMR quadrupole splittings. It is defined by the equation $S_{cd} = \langle {}^3/_2 \cos^2(\theta_{cd}) - {}^1/_2 \rangle$ where θ_{cd} is the angle between the C−H bond vector and the bilayer normal.[73] Figure 7a,b shows the order parameters calculated for the sn2 and sn1 chains of DPPC, respectively, and Figure 7c,d presents the corresponding changes in order parameters for the mixed film systems in comparison with the pure DPPC values.

In the case of both zwitterionic and neutral Phe, the presence of Phe increases the microscopic order of the hydrocarbon chains of the DPPC molecules. In the presence of 20 molecules of zwitterionic Phe, the perturbation of the tails of DPPC is fairly uniform, as evidenced by the nearly constant change in the order parameters (red line, Figure 7c), with a slightly more pronounced effect closest to the headgroup of DPPC. To simulate more realistically the experimental situation, where the macroscopic bulk solution provides a nearly constant supply of

DOI: 10.1021/jp508473w
J. Phys. Chem. B 2015, 119, 9038−9048

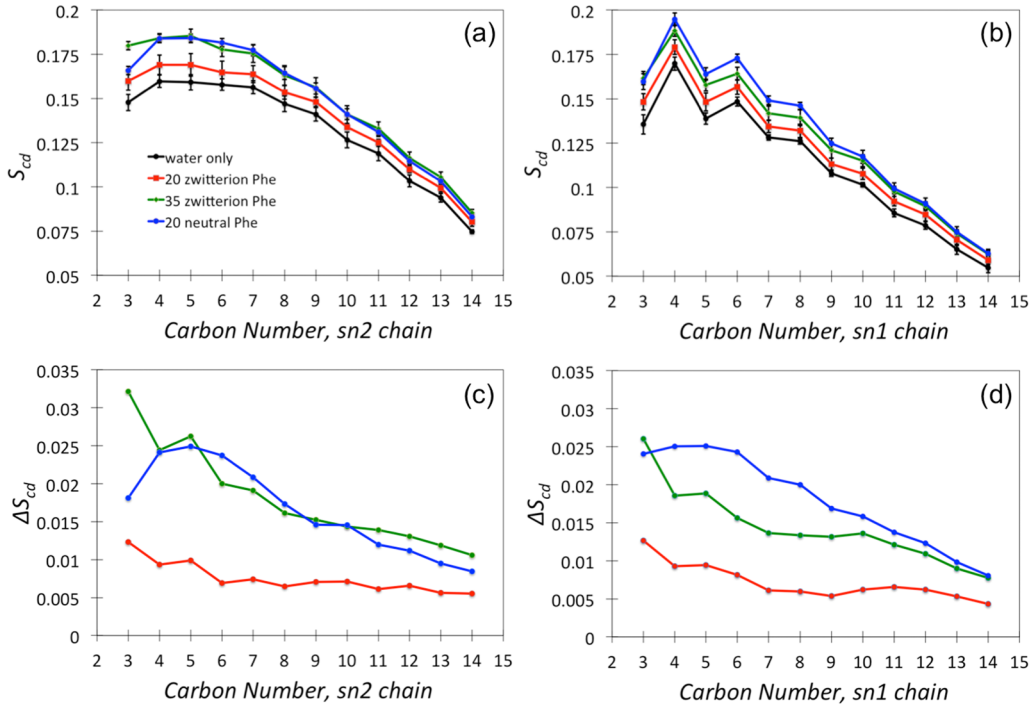

Figure 7. Deuterium order parameters of the (a) sn2 and (b) sn1 chains of DPPC. Color coding: DPPC on a pure water slab (black), in the presence of 20 molecules of zwitterionic Phe (red), with 15 additional zwitterionic Phe molecules added (green), and in the presence of 20 molecules of neutral Phe (blue). Error bars correspond to one standard deviation. In panels (c) and (d), the relative changes in order parameter from those of the DPPC monolayer on a pure water subphase are shown for the sn2 and sn1 chains, respectively.

Phe monomers to the interfacial region to replenish those that have already been partitioned into the monolayer, a subsequent simulation was run with an additional 15 molecules of zwitterionic Phe added to the bulk underneath the DPPC film, yielding a total of 35 molecules of Phe in the simulation. After this addition, there is a much more pronounced effect on the order parameters, with a more distinct perturbation near the headgroup of DPPC, but still with a significant perturbation of the rest of the tail. Finally, in the presence of 20 neutral Phe molecules, there is also a significant increased microscopic ordering of the hydrocarbon tails of DPPC, but now with a maximum effect around carbons 5 and 6 and less of an effect closer to the headgroup. These results are consistent with the density profiles (Figure 3), which showed neutral Phe partitioning deeper into the DPPC film than zwitterionic Phe.

A similar condensing effect on a DPPC film was observed by Chen et al.[15] using BAM in the presence of dimethyl sulfoxide (DMSO), a membrane penetration enhancer used in drug delivery applications. In that study it was observed that DMSO condenses the phospholipid films, resulting in more condensed regions and likely lower surface coverage of phospholipid. This was then suggested to be a contributing factor in the enhanced penetration ability of cells treated with DMSO. Similarly here, in the presence of Phe the DPPC film appears to become more microscopically condensed, yielding some areas of lower DPPC coverage such as the microscopic pore pictured in Figure 6. Additionally the changes in domain morphology observed through BAM are consistent with the picture put forward by Chen et al. as well as the microscopic effects observed through MD simulations. Thus, an ordering of DPPC in the presence of Phe in the interfacial region may contribute to the increased permeability, in a manner similar to DMSO, and destruction of cells as observed in PKU studies.[9]

CONCLUSIONS

By a combination of surface-sensitive experimental techniques and MD simulations, it is shown here that L-phenylalanine does intercalate into a DPPC film at the air−water interface, thereby affecting the surface tension, phase morphology, and ordering of the DPPC film. Phe was not observed to form long fibrils in solution in the experiments or simulations presented here. Rather, Phe was seen to form dynamic small clusters in the simulations, and in the experiments it was shown to have the ability to form needlelike crystals upon drying and supersaturation. Combined with the observation of small aggregates of Phe at the bare water surface using BAM, the interfacial region is suggested to play a role in enhancing the aggregation of Phe. Regardless of the extent of aggregation in the bulk, the effects of Phe on DPPC films, as observed in experiments and simulations, can have a great influence on the permeability and stability of a cell membrane. The experimental Langmuir trough and BAM results illustrate the changes in surface tension and phase behavior. The simulation results further characterize the molecular-level interactions and perturbations of the microscopic ordering of the hydrocarbon chains of DPPC illustrating these changes. In addition, if Phe transitions to its neutral state once it is within the hydrophobic part of the phospholipid phase, the present results show that it has the ability to penetrate deeper within the hydrocarbon core of the DPPC film compared with the zwitterionic form of Phe, enhancing the possibility for embedding into the membrane, membrane crossing events, and increasing local concentration to favor aggregation. In summary, Phe significantly perturbs the structure and morphology of a two-dimensional DPPC film used as a model for a cell membrane through direct Phe−phospholipid interactions and/or membrane-mediated aggregation. This study indicates that it is likely that cytotoxicity in

DOI: 10.1021/jp508473w
J. Phys. Chem. B 2015, 119, 9038−9048

PKU arises from interactions between Phe and the cell membrane. Our results illustrate how Phe affects the membrane structure and stability, which may be applied to many different biological systems.

■ ASSOCIATED CONTENT

Supporting Information

MD simulation insertion procedure and snapshots of Phe adsorption into the DPPC film; confocal microscopy images of Phe fibril formation during droplet drying; BAM images of Phe aggregates at a bare water interface and an unperturbed DPPC film at various surface concentrations; atomic names and charges for neutral and zwitterionic Phe used in MD simulations; and topology files (TXT) for neutral Phe and zwitterionic Phe. This material is available free of charge via the Internet at http://pubs.acs.org.

■ AUTHOR INFORMATION

Corresponding Authors

*E-mail: vaida@colorado.edu. Phone: 303-492-8605. Fax: 303-492-5894.

*E-mail: roesel@uochb.cas.cz. Phone: +420-220-410-313.

Notes

The authors declare no competing financial interest.

■ ACKNOWLEDGMENTS

V.V., E.C.G., and R.J.P. acknowledge a grant from the National Science Foundation (NSF) (CHE-1306386). E.C.G. acknowledges support from a NASA Earth and Space Science Graduate Fellowship. R.J.P. acknowledges support from a CIRES Graduate Fellowship, the Marion L. Sharrah Graduate Fellowship through the CU Chemistry Department, and the NIH/CU Molecular Biophysics Training Program. H.C.A., E.M.A., and D.M.T. acknowledge support from NSF CAICE Grant 45345218. In addition, the authors thank Pavel Jungwirth for helpful discussions and Alena Habartová for technical assistance with MD simulations during a visit of E.C.G. in Prague. M.R. and L.C. acknowledge Grant 13-06181S from the Czech Science Foundation. This work was supported in part by the funding to the Institute of Organic Chemistry and Biochemistry ASCR in Prague via RVO 61388963.

■ REFERENCES

(1) Krzysciak, W. Activity of Selected Aromatic Amino Acids in Biological Systems. *Acta Biochim. Pol.* **2011**, *58*, 461−466.

(2) Hong, H. D.; Park, S.; Jimenez, R. H. F.; Rinehart, D.; Tamm, L. K. Role of Aromatic Side Chains in the Folding and Thermodynamic Stability of Integral Membrane Proteins. *J. Am. Chem. Soc.* **2007**, *129*, 8320−8327.

(3) Domene, C.; Vemparala, S.; Klein, M. L.; Vénien-Bryan, C.; Doyle, D. A. Role of Aromatic Localization in the Gating Process of a Potassium Channel. *Biophys. J.* **2006**, *90*, L01−L03.

(4) Kelkar, D.; Chattopadhyay, A. Membrane Interfacial Localization of Aromatic Amino Acids and Membrane Protein Function. *J. Biosci. (Bangalore)* **2006**, *31*, 297−302.

(5) Gazit, E. A Possible Role for π-Stacking in the Self-Assembly of Amyloid Fibrils. *FASEB J.* **2002**, *16*, 77−83.

(6) Makin, O. S.; Atkins, E.; Sikorski, P.; Johansson, J.; Serpell, L. C. Molecular Basis for Amyloid Fibril Formation and Stability. *Proc. Natl. Acad. Sci. U.S.A.* **2005**, *102*, 315−320.

(7) Marshall, K. E.; Morris, K. L.; Charlton, D.; O'Reilly, N.; Lewis, L.; Walden, H.; Serpell, L. C. Hydrophobic, Aromatic, and Electrostatic Interactions Play a Central Role in Amyloid Fibril Formation and Stability. *Biochemistry* **2011**, *50*, 2061−2071.

(8) Tamamis, P.; Adler-Abramovich, L.; Reches, M.; Marshall, K.; Sikorski, P.; Serpell, L.; Gazit, E.; Archontis, G. Self-Assembly of Phenylalanine Oligopeptides: Insights from Experiments and Simulations. *Biophys. J.* **2009**, *96*, 5020−5029.

(9) Adler-Abramovich, L.; Vaks, L.; Carny, O.; Trudler, D.; Magno, A.; Caflisch, A.; Frenkel, D.; Gazit, E. Phenylalanine Assembly into Toxic Fibrils Suggests Amyloid Etiology in Phenylketonuria. *Nat. Chem. Biol.* **2012**, *8*, 701−706.

(10) Singh, V.; Rai, R. K.; Arora, A.; Sinha, N.; Thakur, A. K. Therapeutic Implication of L-Phenylalanine Aggregation Mechanism and Its Modulation by D-Phenylalanine in Phenylketonuria. *Sci. Rep.* **2014**, *4*, No. 3875.

(11) Gorbenko, G. P.; Kinnunen, P. K. J. The Role of Lipid−Protein Interactions in Amyloid-Type Protein Fibril Formation. *Chem. Phys. Lipids* **2006**, *141*, 72−82.

(12) Coutinho, A.; Loura, L. M. S.; Prieto, M. FRET Studies of Lipid−Protein Aggregates Related to Amyloid-like Fibers. *J. Neurochem.* **2011**, *116*, 696−701.

(13) Griffith, E. C.; Vaida, V. In Situ Observation of Peptide Bond Formation at the Water−Air Interface. *Proc. Natl. Acad. Sci. U.S.A.* **2012**, *109*, 15697−15701.

(14) Chen, X.; Allen, H. C. Interactions of Dimethylsulfoxide with a Dipalmitoylphosphatidylcholine Monolayer Studied by Vibrational Sum Frequency Generation. *J. Phys. Chem. A* **2009**, *113*, 12655−12662.

(15) Chen, X. K.; Huang, Z. S.; Hua, W.; Castada, H.; Allen, H. C. Reorganization and Caging of DPPC, DPPE, DPPG, and DPPS Monolayers Caused by Dimethylsulfoxide Observed Using Brewster Angle Microscopy. *Langmuir* **2010**, *26*, 18902−18908.

(16) Yan, E. C. Y.; Fu, L.; Wang, Z.; Liu, W. Biological Macromolecules at Interfaces Probed by Chiral Vibrational Sum Frequency Generation Spectroscopy. *Chem. Rev.* **2014**, *114*, 8471−8498.

(17) Seoane, R.; Minones, J.; Conde, O.; Casas, M.; Iribarnegaray, E. Thermodynamic and Brewster Angle Microscopy Studies of Fatty Acid/Cholesterol Mixtures at the Air/Water Interface. *J. Phys. Chem. B* **2000**, *104*, 7735−7744.

(18) Berkowitz, M. L.; Bostick, D. L.; Pandit, S. Aqueous Solutions Next to Phospholipid Membrane Surfaces: Insights from Simulations. *Chem. Rev.* **2006**, *106*, 1527−1539.

(19) McConlogue, C. W.; Malamud, D.; Vanderlick, T. K. Interaction of DPPC Monolayers with Soluble Surfactants: Electrostatic Effects of Membrane Perturbants. *Biochim. Biophys. Acta* **1998**, *1372*, 124−134.

(20) Brockman, H. Lipid Monolayers: Why Use Half a Membrane To Characterize Protein−Membrane Interactions? *Curr. Opin. Struct. Biol.* **1999**, *9*, 438−443.

(21) Ma, G.; Allen, H. C. DPPC Langmuir Monolayer at the Air−Water Interface: Probing the Tail and Head Groups by Vibrational Sum Frequency Generation Spectroscopy. *Langmuir* **2006**, *22*, 5341−5349.

(22) Sampaio, J. L.; Gerl, M. J.; Klose, C.; Ejsing, C. S.; Beug, H.; Simons, K.; Shevchenko, A. Membrane lipidome of an epithelial cell line. *Proc. Natl. Acad. Sci. U.S.A.* **2011**, *108*, 1903−1907.

(23) Zuo, Y. Y.; Veldhuizen, R. A. W.; Neumann, A. W.; Petersen, N. O.; Possmayer, F. Current Perspectives in Pulmonary Surfactant—Inhibition, Enhancement and Evaluation. *Biochim. Biophys. Acta* **2008**, *1778*, 1947−1977.

(24) McConlogue, C. W.; Vanderlick, T. K. A Close Look at Domain Formation in DPPC Monolayers. *Langmuir* **1997**, *13*, 7158−7164.

(25) Creuwels, L.; vanGolde, L. M. G.; Haagsman, H. P. The Pulmonary Surfactant System: Biochemical and Clinical Aspects. *Lung* **1997**, *175*, 1−39.

(26) Klopfer, K. J.; Vanderlick, T. K. Isotherms of Dipalmitoylphosphatidylcholine (DPPC) Monolayers: Features Revealed and Features Obscured. *J. Colloid Interface Sci.* **1996**, *182*, 220−229.

(27) Gilman, J. B.; Tervahattu, H.; Vaida, V. Interfacial Properties of Mixed Films of Long-Chain Organics at the Air−Water Interface. *Atmos. Environ.* **2006**, *40*, 6606−6614.

DOI: 10.1021/jp508473w
J. Phys. Chem. B 2015, 119, 9038−9048

(28) Griffith, E. C.; Adams, E. M.; Allen, H. C.; Vaida, V. Hydrophobic Collapse of a Stearic Acid Film by Adsorbed L-Phenylalanine at the Air−Water Interface. *J. Phys. Chem. B* **2012**, *116*, 7849−7857.
(29) Griffith, E. C.; Guizado, T. R. C.; Pimentel, A. S.; Tyndall, G. S.; Vaida, V. Oxidized Aromatic−Aliphatic Mixed Films at the Air−Aqueous Interface. *J. Phys. Chem. C* **2013**, *117*, 22341−22350.
(30) Jubb, A. M.; Hua, W.; Allen, H. C. Environmental Chemistry at Vapor/Water Interfaces: Insights from Vibrational Sum Frequency Generation Spectroscopy. *Annu. Rev. Phys. Chem.* **2012**, *63*, 107−130.
(31) Rontu, N.; Vaida, V. Surface Partitioning and Stability of Pure and Mixed Films of 8−2 Fluorotelomer Alcohol at the Air−Water Interface. *J. Phys. Chem. C* **2007**, *111*, 11612−11618.
(32) Rontu, N.; Vaida, V. Miscibility of Perfluorododecanoic Acid with Organic Acids at the Air−Water Interface. *J. Phys. Chem. C* **2007**, *111*, 9975−9980.
(33) Griffith, E. C.; Vaida, V. Ionization State of L-Phenylalanine at the Air−Water Interface. *J. Am. Chem. Soc.* **2013**, *135*, 710−716.
(34) Henon, S.; Meunier, J. Microsope at the Brewster Angle—Direct Observation of 1st-Order Phase Tranisitions in Monolayers. *Rev. Sci. Instrum.* **1991**, *62*, 936−939.
(35) Honig, D.; Mobius, D. Direct Visualization of Monolayers at the Air−Water Interface by Brewster Angle Microscopy. *J. Phys. Chem.* **1991**, *95*, 4590−4592.
(36) Avdeef, A.; Box, K. J.; Comer, J. E. A.; Hibbert, C.; Tam, K. Y. pH-Metric logP 10. Determination of Liposomal Membrane−Water Partition Coefficients of Ionizable Drugs. *Pharm. Res.* **1998**, *15*, 209−215.
(37) MacCallum, J. L.; Bennett, W. F. D.; Tieleman, D. P. Distribution of Amino Acids in a Lipid Bilayer from Computer Simulations. *Biophys. J.* **2008**, *94*, 3393−3404.
(38) Nosé, S. A Molecular-Dynamics Method for Simulations in the Canonical Ensemble. *Mol. Phys.* **1984**, *52*, 255−268.
(39) Hoover, W. G. Canonical Dynamics: Equilibrium Phase-Space Distributions. *Phys. Rev. A* **1985**, *31*, 1695−1697.
(40) Hockney, R. W.; Goel, S. P.; Eastwood, J. W. Quiet High-Resolution Computer Models of a Plasma. *J. Comput. Phys.* **1974**, *14*, 148−158.
(41) Darden, T.; York, D.; Pedersen, L. Particle Mesh Ewald: An *N*·log(*N*) Method for Ewald Sums in Large Systems. *J. Chem. Phys.* **1993**, *98*, 10089−10092.
(42) Hess, B.; Bekker, H.; Berendsen, H. J. C.; Fraaije, J. G. E. M. LINCS: A Linear Constraint Solver for Molecular Simulations. *J. Comput. Chem.* **1997**, *18*, 1463−1472.
(43) Hess, B.; Kutzner, C.; van der Spoel, D.; Lindahl, E. GROMACS 4: Algorithms for Highly Efficient, Load-Balanced, and Scalable Molecular Simulation. *J. Chem. Theory Comput.* **2008**, *4*, 435−447.
(44) Humphrey, W.; Dalke, A.; Schulten, K. VMD: Visual Molecular Dynamics. *J. Mol. Graphics* **1996**, *14*, 33−38.
(45) Jämbeck, J. P. M.; Lyubartsev, A. P. Derivation and Systematic Validation of a Refined All-Atom Force Field for Phosphatidylcholine Lipids. *J. Phys. Chem. B* **2012**, *116*, 3164−3179.
(46) Jämbeck, J. P. M.; Lyubartsev, A. P. An Extension and Further Validation of an All-Atomistic Force Field for Biological Membranes. *J. Chem. Theory Comput.* **2012**, *8*, 2938−2948.
(47) Klauda, J. B.; Venable, R. M.; Freites, J. A.; O'Connor, J. W.; Tobias, D. J.; Mondragon-Ramirez, C.; Vorobyov, I.; MacKerell, A. D.; Pastor, R. W. Update of the CHARMM All-Atom Additive Force Field for Lipids: Validation on Six Lipid Types. *J . Phys. Chem. B* **2010**, *114*, 7830−7843.
(48) Duan, Y.; Wu, C.; Chowdhury, S.; Lee, M. C.; Xiong, G.; Zhang, W.; Yang, R.; Cieplak, P.; Luo, R.; Lee, T.; et al. A Point-Charge Force Field for Molecular Mechanics Simulations of Proteins Based on Condensed-Phase Quantum Mechanical Calculations. *J. Comput. Chem.* **2003**, *24*, 1999−2012.
(49) Lee, M. C.; Duan, Y. Distinguish Protein Decoys by Using a Scoring Function Based on a New Amber Force Field, Short Molecular Dynamics Simulations, and the Generalized Born Solvent Model. *Proteins: Struct., Funct., Bioinf.* **2004**, *55*, 620−634.
(50) Bayly, C. I.; Cieplak, P.; Cornell, W. D.; Kollman, P. A. A Well-Behaved Electrostatic Potential Based Method Using Charge Restraints for Deriving Atomic Charges—The RESP Model. *J. Phys. Chem.* **1993**, *97*, 10269−10280.
(51) Tomasi, J.; Mennucci, B.; Cancès, E. The IEF Version of the PCM Solvation Method: An Overview of a New Method Addressed To Study Molecular Solutes at the QM Ab Initio Level. *J. Mol. Struct.: THEOCHEM* **1999**, *464*, 211−226.
(52) Frisch, M. J.; Trucks, G. W.; Schlegel, H. B.; Scuseria, G. E.; Robb, M. A.; Cheeseman, J. R.; Scalmani, G.; Barone, V.; Mennucci, B.; Petersson, G. A.; et al. *Gaussian 09*; Gaussian, Inc.: Wallingford, CT, 2009.
(53) Wang, J. M.; Wang, W.; Kollman, P. A.; Case, D. A. Automatic Atom Type and Bond Type Perception in Molecular Mechanical Calculations. *J. Mol. Graphics Modell.* **2006**, *25*, 247−260.
(54) Williams, R. A.; Mamotte, C. D. S.; Burnett, J. R. Phenylketonuria: An Inborn Error of Phenylalanine Metabolism. *Clin. Biochem. Rev.* **2008**, *29*, 31−41.
(55) Petrache, H. I.; Dodd, S. W.; Brown, M. F. Area Per Lipid and Acyl Length Distributions in Fluid Phosphatidylcholines Determined by ^{2}H NMR Spectroscopy. *Biophys. J.* **2000**, *79*, 3172−3192.
(56) López-Montero, I.; Vélez, M.; Devaux, P. F. Surface Tension Induced by Sphingomyelin to Ceramide Conversion in Lipid Membranes. *Biochim. Biophys. Acta* **2007**, *1768*, 553−561.
(57) Dolowy, K. 275 - Effect of Interfacial Tension and Curvature of Charged Lipid Bilayer−Polylysine Complexes. *Bioelectrochem. Bioenerg.* **1979**, *6*, 305−307.
(58) Andrews, C. T.; Elcock, A. H. Molecular Dynamics Simulations of Highly Crowded Amino Acid Solutions: Comparisons of Eight Different Force Field Combinations with Experiment and with Each Other. *J. Chem. Theory Comput.* **2013**, *9*, 4585−4602.
(59) Zhou, X.; Fan, J.; Li, N.; Du, Z.; Ying, H.; Wu, J.; Xiong, J.; Bai, J. Solubility of L-Phenylalanine in Water and Different Binary Mixtures from 288.15 to 318.15 K. *Fluid Phase Equilib.* **2012**, *316*, 26−33.
(60) Eisenthal, K. B. Liquid Interfaces Probed by Second-Harmonic and Sum-Frequency Spectroscopy. *Chem. Rev.* **1996**, *96*, 1343−1360.
(61) Donaldson, D. J.; Vaida, V. The Influence of Organic Films at the Air−Aqueous Boundary on Atmospheric Processes. *Chem. Rev.* **2006**, *106*, 1445−1461.
(62) Vaida, V. Perspective: Water Cluster Mediated Atmospheric Chemistry. *J. Chem. Phys.* **2011**, *135*, No. 020901.
(63) Lee, H. J.; Choi, C.; Lee, S. J. Membrane-Bound α-Synuclein Has a High Aggregation Propensity and the Ability To Seed the Aggregation of the Cytosolic Form. *J. Biol. Chem.* **2002**, *277*, 671−678.
(64) Knight, J. D.; Miranker, A. D. Phospholipid Catalysis of Diabetic Amyloid Assembly. *J. Mol. Biol.* **2004**, *341*, 1175−1187.
(65) Choo-Smith, L. P.; Garzon-Rodriguez, W.; Glabe, C. G.; Surewicz, W. K. Acceleration of Amyloid Fibril Formation by Specific Binding of Aβ-(1−40) Peptide to Ganglioside-Containing Membrane Vesicles. *J. Biol. Chem.* **1997**, *272*, 22987−22990.
(66) Morriss-Andrews, A.; Brown, F. L. H.; Shea, J. E. A Coarse-Grained Model for Peptide Aggregation on a Membrane Surface. *J. Phys. Chem. B* **2014**, *118*, 8420−8432.
(67) Fu, L.; Ma, G.; Yan, E. C. Y. In Situ Misfolding of Human Islet Amyloid Polypeptide at Interfaces Probed by Vibrational Sum Frequency Generation. *J. Am. Chem. Soc.* **2010**, *132*, 5405−5412.
(68) Dyson, H. J.; Wright, P. E. Intrinsically Unstructured Proteins and Their Functions. *Nat. Rev. Mol. Cell Biol.* **2005**, *6*, 197−208.
(69) Tompa, P. Intrinsically Unstructured Proteins. *Trends Biochem. Sci.* **2002**, *27*, 527−533.
(70) Uversky, V. N. Natively Unfolded Proteins: A Point Where Biology Waits for Physics. *Protein Sci.* **2002**, *11*, 739−756.
(71) Knecht, V.; Müller, M.; Bonn, M.; Marrink, S.-J.; Mark, A. E. Simulation Studies of Pore and Domain Formation in a Phospholipid Monolayer. *J. Chem. Phys.* **2005**, *122*, No. 024704.
(72) Chau, P. L.; Hardwick, A. J. A New Order Parameter for Tetrahedral Configurations. *Mol. Phys.* **1998**, *93*, 511−518.

DOI: 10.1021/jp508473w
J. Phys. Chem. B 2015, 119, 9038−9048

(73) Schindler, H.; Seelig, J. Deuterium Order Parameters in Relation to Thermodynamic Properties of a Phospholipid Bilayer. A Statistical Mechanical Interpretation. *Biochemistry* **1975**, *14*, 2283−2287.

DOI: 10.1021/jp508473w
J. Phys. Chem. B 2015, 119, 9038−9048